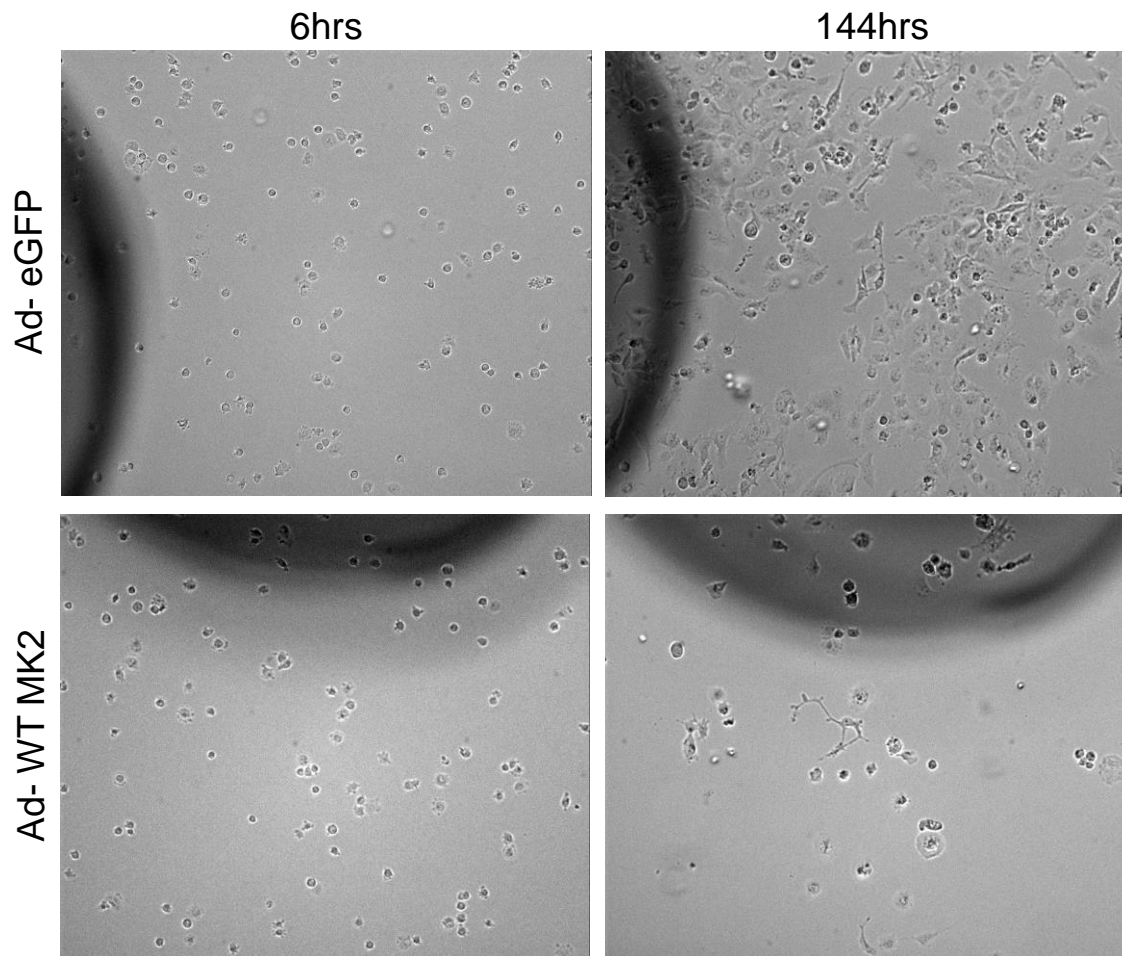
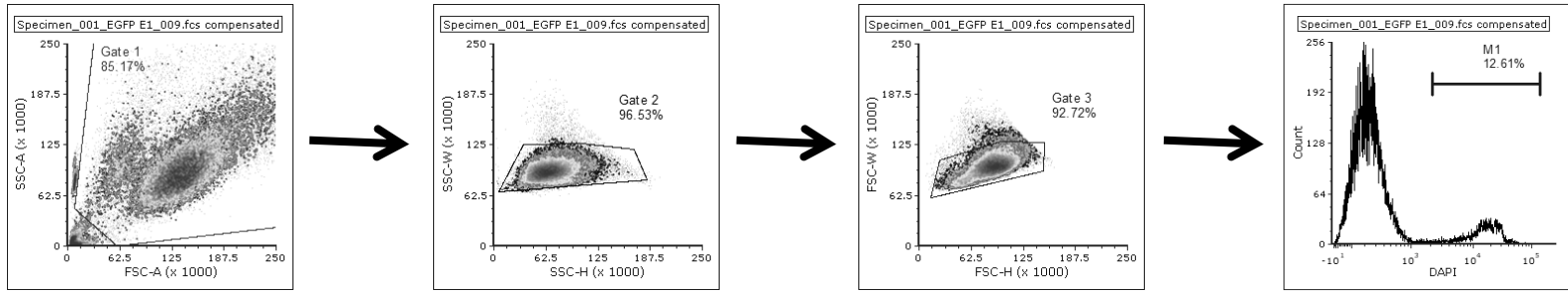


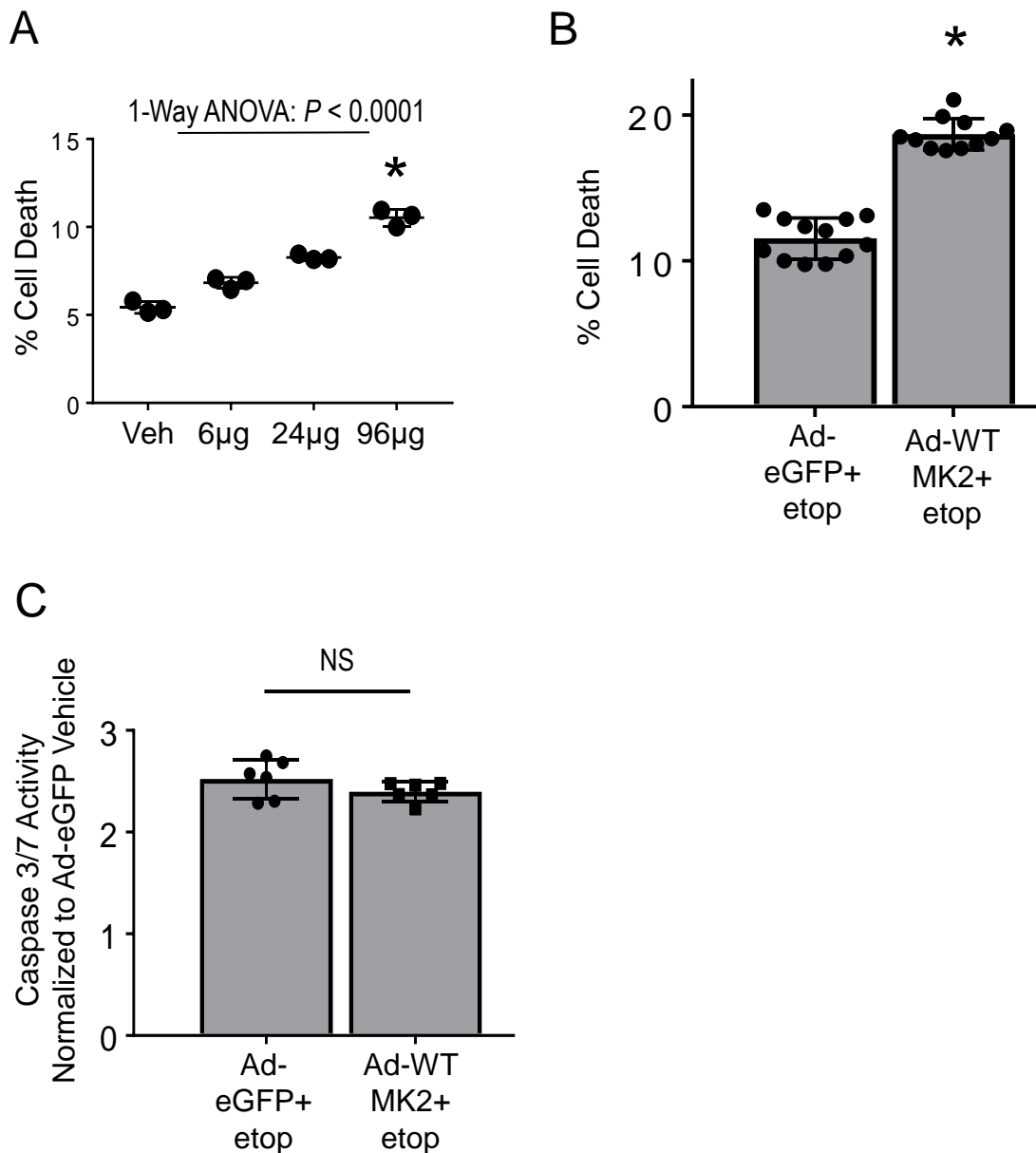
Supplemental Figure 1: Schematic representation of MK2 (1-400 a.a.) protein structure. At N-terminal domain contains a proline-rich region (10–40 a.a.) followed by catalytic kinase domain (64–325 a.a.). The C-terminal domain consists of a nuclear export signal (NES) (356–365 a.a.) and a bipartite nuclear localization signal (NLS) (371–374 and 385–389 a.a.). Brown color, amino acid substitution for dominant negative MK2 mutant construct. Green color, amino acid substitutions for constitutively active MK2 mutant construct. Red color, amino acid substitution for nuclear export sequence mutant MK2 variant. Blue color, amino acid substitutions for nuclear localization sequence mutant MK2 variant.



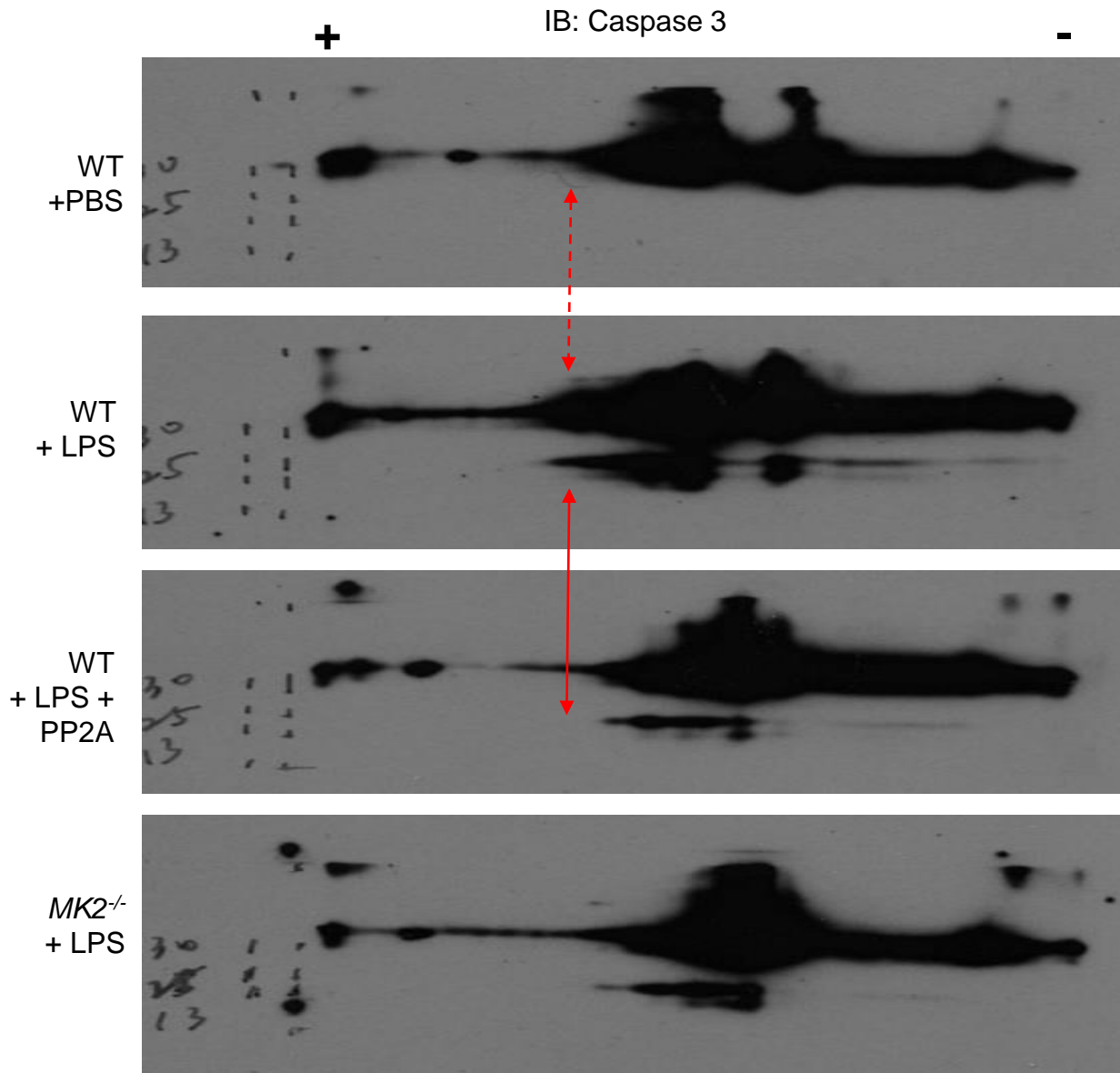
Supplemental Figure 2: Time lapse bright-field microscopy was used to show the effect of MK2 expression on H23 cells. Six hours after sub-confluent plating, H23 cells were infected with Ad-eGFP or Ad-WT MK2 and imaged over time, up to 144hrs. Images show H23 cells infected with Ad-eGFP continue to proliferate to confluency at 144hrs. However, H23 cells infected with Ad-WT MK2 fail to grow to confluency and appear less populated at 144hrs than at 6hrs.



Supplemental Figure 3: Gating strategy for detecting cell death. Gating strategy to identify apoptotic H23 cells. Forward and side scatter (FSC and SSC) gating on area (A), height (H), and width (W) excluded debris and non-single cell events. Then relative fluorescence of DAPI staining was measured. The amount of positive DAPI fluorescent staining was quantified.



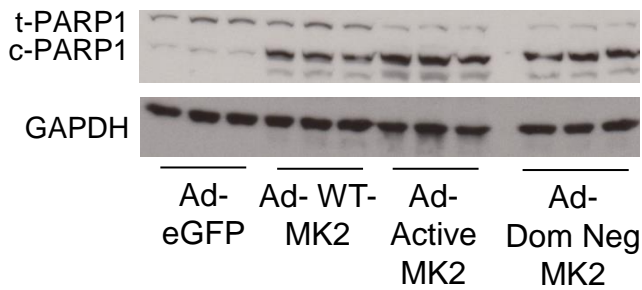
Supplemental Figure 4: Synergistic role of MK2 expression and etoposide on cell death. **A.** H23 cells were exposed to etoposide at varying concentrations for 24hrs followed by staining with DAPI and cell death was assessed using flow cytometry. There is a dose dependent increase in cell death in response to etoposide with 96ug/mL resulting in the highest amount of death. *, $P < 0.05$ vs all other conditions using Dunnett's multiple comparison test. **B-C.** H23 cells were infected with Ad-eGFP or Ad-WT MK2 for 24 hours and then treated with etoposide 96ug/mL for 24hrs. Cells were then analyzed for cell death using flow cytometry (**B**) and caspase 3 activity (**C**). As shown, there is significant increase in cell death with Ad-WT MK2 but not in caspase 3 activity. *, $P < 0.05$ vs Ad-eGFP.



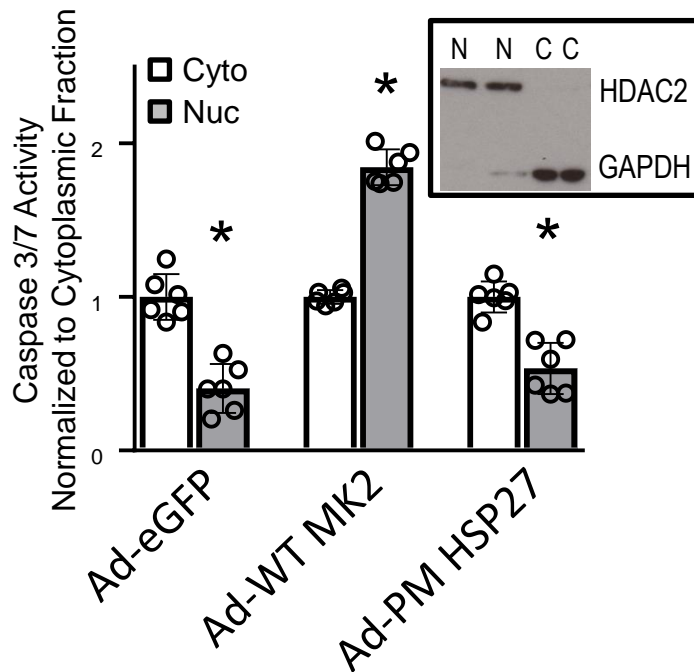
Supplemental Figure 5: MK2 dependent phosphorylation of caspase 3 in mouse lung tissue.

Lung homogenates from wild-type and $MK2^{-/-}$ mice exposed to PBS or LPS (IV 7.5mg/kg, 6hrs) were treated with or without the serine/threonine phosphatase PP2A and underwent 2-Dimensional immunoblotting for caspase 3. As shown, there is a shift toward the positive electrode on an isoelectric gradient in lung homogenates from WT animals exposed to LPS (Red Dash Arrow). Treatment of lung homogenates from WT animals exposed to LPS with active recombinant serine/threonine phosphatase, PP2A, reverses these charge based shifts (red arrow), suggestive of a LPS-induced phosphorylation event. Additionally, 2-Dimensional immunoblotting for caspase 3 of lung homogenates from $MK2^{-/-}$ mice exposed to LPS appears similar to that of lung homogenates from WT animals exposed to LPS and treated with active recombinant PP2A, suggestive of a MK2-dependent phosphorylation event on caspase 3. Representative immunoblots from 3 mice/group.

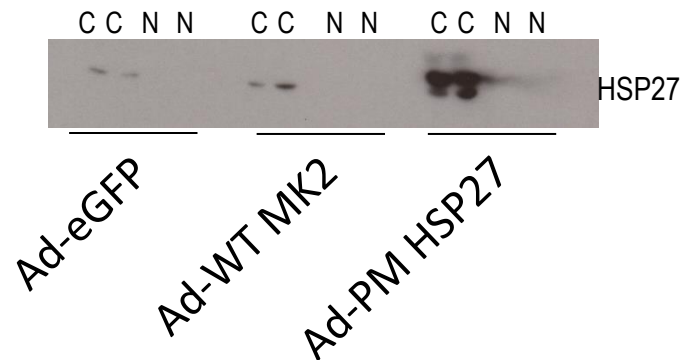
A



B

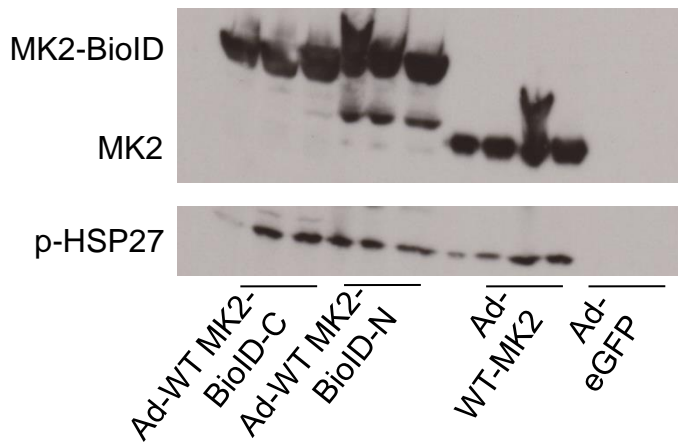


C

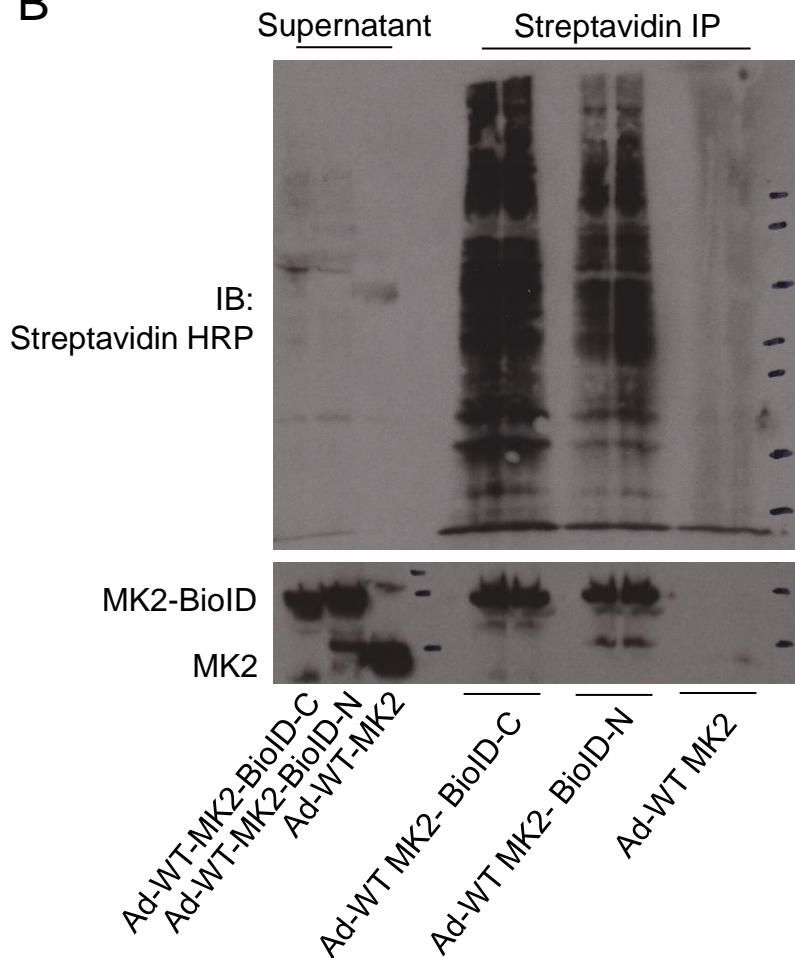


Supplemental Figure 6: Nuclear translocation of caspase 3 is independent of MK2 activity. **A.** H23 NSCLC cells were infected with Ad-eGFP, Ad-WT-MK2, Ad-Active-MK2 or Ad-Dom Neg-MK2 for 48hrs and then harvested for protein analyses. Representative immunoblot indicates an increase in cleavage of PARP1, a nuclear substrate of caspase 3, in Ad-WT MK2, Ad-Active-MK2 and Ad-Dom Neg-MK2 infected H23 cells compared to Ad-eGFP infected H23 cells. **B.** H23 NSCLC cells were infected with Ad-eGFP, Ad-WT-MK2, Ad-PM HSP27 for 48hrs and then nuclear and cytoplasmic fractions were generated for assessment of caspase 3 activity. Infection of H23 cells with Ad-WT MK2 results in increased nuclear caspase 3 activity; whereas infection with Ad-eGFP (control virus) or Ad-PM HSP27 (phospho-mimicking HSP27, the immediate downstream target of MK2) demonstrates significantly reduced nuclear caspase 3 activity compared to cytoplasmic. **C.** H23 NSCLC cells were infected with Ad-eGFP, Ad-WT-MK2, Ad-PM HSP27 for 48hrs and then nuclear and cytoplasmic fractions were generated for protein analyses. Representative immunoblot marked expression of HSP27 with a higher molecular weight, indicating phosphorylation.

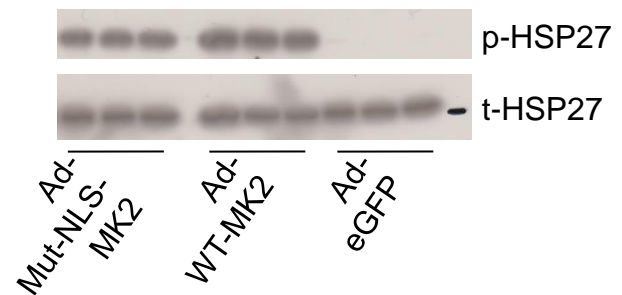
A



B



C



Supplemental Figure 7: Validation of MK2 constructs. H23 cells were infected with Ad-WT-MK2, Ad-WT MK2-BioID-C (MK2 fused to biotin ligase on the c-terminus) or Ad-WT MK2-BioID-N (MK2 fused to biotin ligase on the n-terminus) and following incubation with biotin, cell lysates were precipitated with beads conjugated to streptavidin and then subjected to immunoblotting. **A:** There is an increase in molecular weight of MK2 when conjugated to biotin ligase, as shown by the shift in the immunoreactive band. There is also phosphorylation of HSP27 in cells infected with Ad-WT-MK2, Ad-WT MK2-BioID-C or Ad-WT MK2-BioID-N, demonstrating the addition of the biotin ligase did not impact its kinase function. **B.** Purity of streptavidin pull downs is demonstrated by minimal immunoreactivity in the supernatants and in lysates infected with Ad-WT-MK2. **C.** Representative immunoblot of lysates from H23 cells infected with Ad-eGFP, Ad-WT MK2 or Ad-Mut-NLS-MK2 for 48 hours demonstrates phosphorylation of HSP27 in cells infected with Ad-WT MK2 or Ad-Mut-NLS-MK2, demonstrating retention of MK2's kinase activity with the mutation within the NLS.